



Review

Spectroscopic Ellipsometry: Advancements, Applications and Future Prospects in Optical Characterization

Grazia Giuseppina Politano ^{1,*} and Carlo Versace ^{2,3}

¹ Department of Information Engineering, Infrastructures and Sustainable Energy (DIIES), University "Mediterranea" of Reggio Calabria, 89122 Reggio Calabria, Italy

² Dipartimento di Fisica, Università della Calabria, 87036 Rende, Italy; carlo.versace@fis.unical.it

³ Licryl CNR/Nanotec c/o, Dipartimento di Fisica, Università della Calabria, 87036 Rende, Italy

* Correspondence: grazia.politano@unirc.it

Abstract: Spectroscopic ellipsometry (SE), a non-invasive optical technique, is a powerful tool for characterizing surfaces, interfaces, and thin films. By analyzing the change in the polarization state of light upon reflection or transmission through a sample, ellipsometry provides essential parameters such as thin film thickness (t) and optical constants (n, k). This review article discusses the principles of ellipsometry, including the measurement of key values Δ and Ψ , and the complex quantity ρ . The article also presents the Fresnel equations for s and p polarizations and the importance of oblique angles of incidence in ellipsometry. Data analysis in ellipsometry is explored, including the determination of bandgap and data referencing the electrical properties of materials. The article emphasizes the importance of choosing the appropriate models to fit ellipsometric data accurately, with examples of the Cauchy and Lorentz models. Additionally, the Kramers–Kronig relations are introduced, illustrating the connection between real and imaginary components of optical constants. The review underscores the significance of ellipsometry as a non-destructive and versatile technique for material characterization across a wide range of applications.

Keywords: spectroscopic ellipsometry; refraction index; optical technique



Citation: Politano, G.G.; Versace, C. Spectroscopic Ellipsometry: Advancements, Applications and Future Prospects in Optical Characterization. *Spectrosc. J.* **2023**, *1*, 163–181. <https://doi.org/10.3390/spectroscj1030014>

Academic Editors: Clemens Burda

Received: 17 August 2023

Revised: 3 December 2023

Accepted: 4 December 2023

Published: 6 December 2023



Copyright: © 2023 by the authors. Licensee MDPI, Basel, Switzerland. This article is an open access article distributed under the terms and conditions of the Creative Commons Attribution (CC BY) license (<https://creativecommons.org/licenses/by/4.0/>).

1. Introduction

In the vast field of optical characterization, spectroscopic ellipsometry (SE) emerges as a potent and indispensable technique. It plays a critical role in revealing the optical properties and thicknesses of various materials, with widespread applications spanning a myriad of scientific areas. This review is deliberately designed to be an initial overview of SE, targeting principally those who are new or nurturing a growing interest in SE. The goal is to elucidate its basic principles, methodologies, and diverse applications.

We have incorporated references to detailed reviews authored by esteemed experts in the field of SE (see, for example [1,2]). This inclusion is meticulously designed for readers who aspire to a profound and advanced understanding of SE technique.

2. Theoretical Foundations of Spectroscopic Ellipsometry

Spectroscopic ellipsometry (SE), a non-invasive optical technique, plays a crucial role in characterizing surfaces, interfaces, and thin films. By analyzing the change in the polarization state of light upon reflection or transmission through a sample, ellipsometry derives essential parameters like thin film thickness (t) and optical constants (n, k) from the measurement. The technique derives information from each layer that interacts with the incident light beam. The name “ellipsometry” stems from the fact that polarized light often becomes elliptical after reflection [3].

Two key values, Δ and Ψ , are measured by ellipsometry. These quantities are dependent on wavelength and angle of incidence, and are defined as follows [4]:

$$\tan \psi = \frac{|R^p|}{|R^s|} \tag{1}$$

$$\Delta = \delta_p - \delta_s \tag{2}$$

Ψ represents the angle whose tangent gives the ratio of amplitude attenuation (or magnification) upon reflection for p and s polarizations, with values ranging from zero to 90° . On the other hand, Δ represents the difference between the phase shifts experienced upon reflection by p and s polarizations, with values ranging from zero to 360° . Here, p and s refer to the plane of incidence and the direction perpendicular to it, respectively.

The complex quantity ρ , defined as the complex ratio of the total reflection coefficients, plays a critical role [5].

$$\rho = \tan(\psi)e^{i\Delta} = \frac{\widetilde{R}_p}{\widetilde{R}_s} \tag{3}$$

The capital R implies that the actual material structure can be multilayered and/or multicomponent, making it possible to analyze rough surfaces, interfaces, and layers containing material mixtures [6].

The simplest ellipsometry systems are depicted in Figures 1 and 2 [7,8].

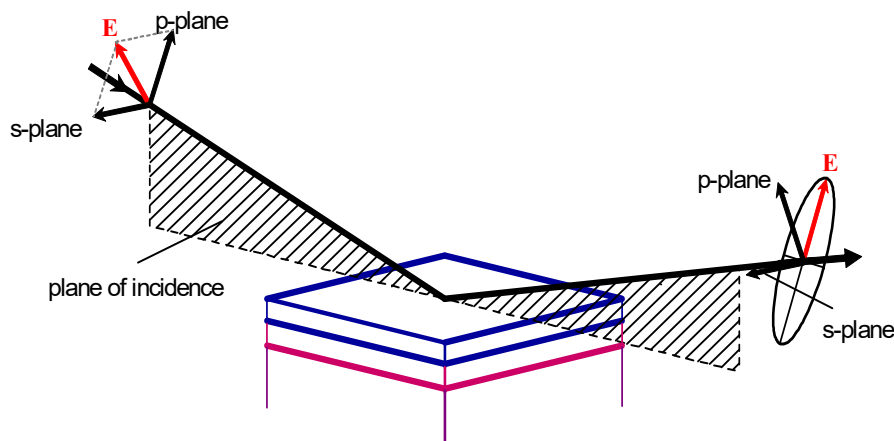


Figure 1. Ellipsometry system [7].

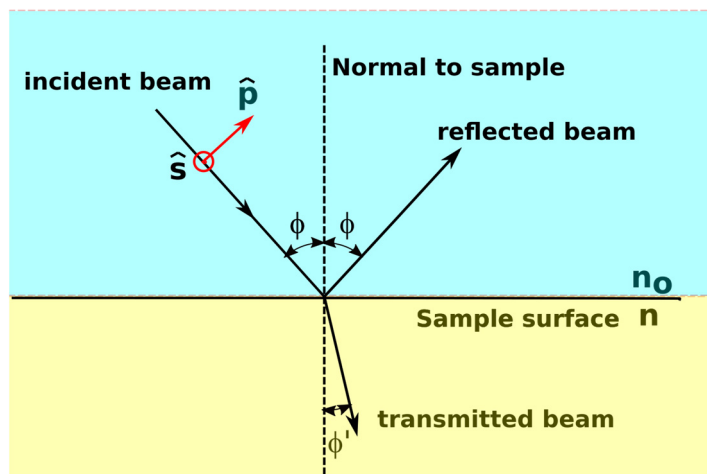


Figure 2. Illustration depicting a monochromatic polarized light beam interacting with a material medium as it approaches from an angle denoted as $\sim \phi$ within an air environment.

In Figure 1 an elliptically polarized light beam hits the sample surface at a certain angle. Its polarization is decomposed into a p component, parallel to the plane of incidence and an s component perpendicular to the plane of incidence. The change in polarization of the reflected ray is measured by analyzing its s and p components.

In Figure 2 is shown a linearly polarized monochromatic light beam incident on a sample at an angle ϕ to the normal. The light polarization can be considered to have vector components in the plane of incidence (p polarization) and a component s perpendicular to it. By applying Maxwell's equations to the boundary between the sample and the incident medium, we derive the Fresnel equations for s and p polarizations determined in (4) [8]:

$$r_p = \frac{n \cos \phi - n_0 \cos \phi'}{n \cos \phi + n_0 \cos \phi'} \frac{E_p^{Ref}}{E_p^{In}} \quad (4)$$

$$r_s = \frac{n_0 \cos \phi - n \cos \phi'}{n_0 \cos \phi + n \cos \phi'} \frac{E_s^{Ref}}{E_s^{In}}$$

Here, E represents the electric field strength for the incident or reflected waves, and n and n_0 are the complex indices of refraction of the sample and the incident medium, respectively. The imaginary part of n is k , the extinction coefficient. The internal angle ϕ is related to ϕ' by Snell's law:

$$n_0 \sin \phi = n \sin \phi' \quad (5)$$

Ellipsometry measures the ratio defined as:

$$\rho = \tan(\psi) e^{i\Delta} = \frac{R_p}{R_s} \quad (6)$$

Inverting Equations (4)–(6) gives:

$$n = n_0 \tan \phi \sqrt{1 - 4\rho(1 + \rho)^{-2} \sin^2 \phi} \quad (7)$$

Since inverting the Fresnel equations for real systems can be challenging, one approach used for materials analysis by ellipsometry is to experimentally acquire ψ and Δ over a wide range of wavelengths and angles of incidence ϕ . These data can then be compared with ψ and Δ calculated for an assumed model for the material under study [8].

Ellipsometry measurements are typically acquired at oblique angles of incidence, usually ranging from 45° to 80° with respect to the sample's surface normal. For instance, when polarized light reflects from an isotropic material, the s -polarized light increases with the angle of incidence, while the p -polarized light goes through a minimum at the Brewster angle before climbing back up, as shown in Figure 3 for a coated glass slide.

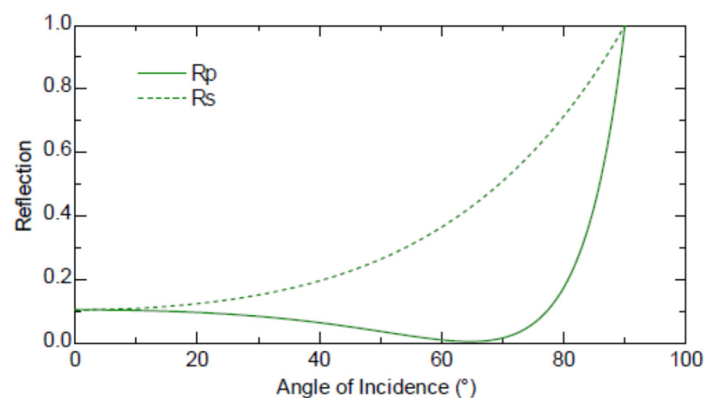


Figure 3. Reflected intensities for both p - and s -polarized light for a coated glass slide [7].

The Fresnel equations predict that light with p polarization will not be reflected if the angle of incidence is

$$\theta_B = \arctan\left(\frac{n_2}{n_1}\right) \quad (8)$$

where n_1 is the refractive index of the incident medium, and n_2 is the index of the other medium. The equation described herein is known as Brewster's law, and the specific angle it defines is referred to as Brewster's angle.

Although modern ellipsometers include a compensator, allowing precise measurements over a wide range of angles, it is still essential to use oblique angles for common ellipsometry applications, as the change in polarization becomes negligible at angles near normal incidence [7].

3. Data Analysis

In the study of materials using ultraviolet/visible region measurements, ellipsometry plays a crucial role in characterizing interband transitions (band structures). Specifically, it allows us to deduce the bandgap (E_g) by observing the variation of α (absorption coefficient) with photon energy ($h\nu$). In the infrared region, ellipsometry provides valuable insights into free carrier absorption induced by free electrons or holes in solids. This enables us to study electrical properties like carrier mobility, carrier concentration, and conductivity [9]. Moreover, ellipsometry in the infrared region allows us to investigate lattice vibration modes (LO and TO phonons) and local atomic structures [10].

For bulk materials, ellipsometry measurements can provide "pseudo" optical constants using the following equation [7]:

$$\langle \bar{\epsilon} \rangle = \sin^2(\phi) \left[1 + \tan^2(\phi) \left(\frac{1 - \rho}{1 + \rho} \right)^2 \right] \quad (9)$$

However, it is important to note that in actual bulk materials, surface oxide or roughness is typically present, which would influence the inversion of this equation. For more complex samples, such as those with multiple layers, inhomogeneity, and surface roughness, experimental ellipsometric angles collected at different incidence angles and photon energies must be compared with those provided by an appropriate model. In Figure 4, a flow chart detailing the process of ellipsometry data analysis is presented.

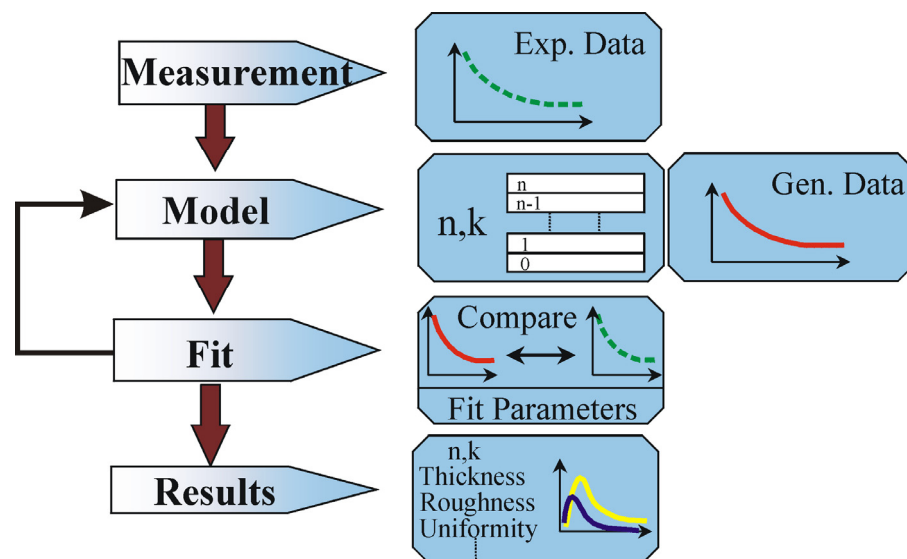


Figure 4. Model used to calculate the predicted response from Fresnel's equations [7].

The process begins with the execution of measurements. The model is then used to calculate the predicted determinations from Fresnel's equations, which describe each material's thickness and optical constants. In cases where these values are unknown, an estimate is used for preliminary calculations. The generated values (red lines in Figure 4) are then compared to the experimental data (green lines) using the mean square error (MSE) as a figure of merit to measure the fit quality [11]. At the end of the process, we observe the resulting optical constants n and k , depicted in Figure 4 in blue and yellow lines. However, it's important to note that other quantities, such as surface roughness, can also be derived from ellipsometry data.

$$MSE = \sqrt{\frac{1}{2N - M} \sum_{i=1}^N \left[\left(\frac{(\psi_i^{mod} - \psi_i^{exp})}{\sigma_{\psi,i}^{exp}} \right)^2 + \left(\frac{(\Delta_i^{mod} - \Delta_i^{exp})}{\sigma_{\Delta,i}^{exp}} \right)^2 \right]} \quad (10)$$

An additional technique known as effective medium approximation (EMA) allows two or three materials to combine and form an "effective" mixed layer, providing a way to describe surface or interfacial roughness, porous layers, and polycrystalline materials [12,13].

SE provides several advantages compared to basic intensity-based measurements. It is non-contact and non-destructive, and it provides fast data acquisition, making it ideal for scientific research (ex situ technique) due to its ability to simulate and generate application models for a wide range of materials, including unknown combinations [14]. However, there are limitations to consider. The spot size of the light beam used in spectroscopic ellipsometry is relatively large, leading to low spatial resolution. This makes it challenging to characterize thin films, specifically, those with thicknesses <10 nm, as the distinction between layer and substrate becomes difficult. Additionally, measuring at small absorption coefficients ($\alpha < 100 \text{ cm}^{-1}$), especially in the ultraviolet region, presents difficulties. Surface roughness must be limited to avoid light depolarization and ensure the applicability of EMA in Bruggeman approximation.

Performing measurements at oblique incidence is necessary, especially in the case of semiconductors (angles of incidence between 50 and 80°) [7]. However, optimizing the incidence angle can be challenging, especially for materials with multiple phases or amorphous structures. Moreover, thin films must have a uniform thickness for accurate ellipsometric measurements. When dealing with multilayer samples, having some prior knowledge of optical constants is beneficial for the initial iteration, as using dielectric functions becomes more complex.

In cases where questionable results are obtained from ellipsometric modeling, corroborating the findings with data from other experiments, such as atomic-force microscopy or XRD, is advisable. This approach ensures a more robust and reliable material characterization.

4. Interaction of Light and Materials

4.1. Index of Refraction

The electromagnetic wave is characterized by both electric and magnetic field vectors that are mutually perpendicular and perpendicular to the direction of wave propagation. While it can be represented using either the magnetic or electric field vector, for simplicity, we will focus on the electric vector. Mathematically, the light wave can be described as follows [3]:

$$A = A_0 \sin \left(-\frac{2\pi}{\lambda} (x - vt) + \zeta \right) \quad (11)$$

Here, A represents the electric field strength at any given time or place, with A_0 denoting the maximum field strength, known as the "amplitude." The variables x , t , v , λ , and ζ represent the distance along the wave's direction of travel, time, velocity of light, wavelength, and an arbitrary phase angle, respectively.

In Figure 5, an electromagnetic wave is depicted.

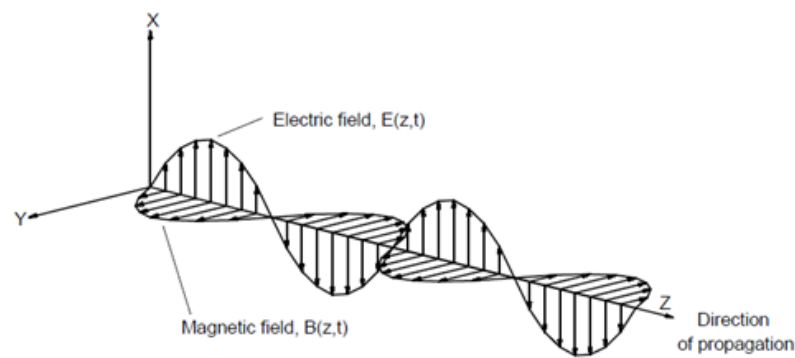


Figure 5. An electromagnetic wave [7].

The complex index of refraction \tilde{N} is a parameter used to describe the interaction of light with materials. It comprises a real part (n) and an imaginary part (k), given as

$$\tilde{N} = n - ik \quad (12)$$

The real part (n) is often referred to as the “index of refraction,” while the imaginary part (k) is known as the “extinction coefficient.” For dielectric materials like glass, the extinction coefficient (k) is zero, and we focus solely on the index of refraction (n). The velocity of light (c) in a vacuum is approximately 3.00×10^8 m/s. However, when light enters a different medium, its velocity (v) changes, and the refractive index (n) is defined as the ratio between the speed of light in a vacuum and its speed in the material, i.e.,

$$n = \frac{c}{v} \quad (13)$$

Transparent media entirely rely on the refractive index (n) to determine the propagation of electromagnetic waves. Nevertheless, there are materials where strong light absorption occurs, and the refractive index (n) alone cannot explain this phenomenon. This is where the extinction coefficient (k) comes into play, which indicates how rapidly the intensity decreases as light travels through the material [3].

The imaginary part of the complex index (the extinction coefficient, k) plays a crucial role in determining the behavior of light in an absorbing medium. If the extinction coefficient (k) is non-zero, the wave’s amplitude will exponentially decay as it propagates along the z -direction. This decay is described by the following expression [15]:

$$E \propto e^{-\frac{2\pi kz}{\lambda}} \quad (14)$$

where z represents the distance of propagation and λ denotes the wavelength, both measured in length units. The wave will decay to $1/e$ of its original amplitude after propagating a distance known as the penetration depth (D_p), which is given by (15). Generally, the wave is considered to be totally absorbed at four penetration depths [3].

$$D_p = \frac{\lambda}{4\pi k} \quad (15)$$

The absorption coefficient (α), which is essential in describing the behavior of light in an absorbing medium, can be related to the extinction coefficient (k) by the equation

$$\alpha = \frac{4\pi k}{\lambda} \quad (16)$$

In a medium that absorbs light, the reduction in intensity I per unit length z is directly proportional to I itself. Mathematically, this relationship is represented by the following expression [3]:

$$\frac{dI(z)}{dz} = -\alpha I(z) \quad (17)$$

By integrating this equation, we can derive

$$I(z) = I_0 e^{-\alpha z} \quad (18)$$

where I_0 is the intensity of the light beam at the medium's entrance, and α only accounts for the loss due to absorption.

4.2. Dielectric Function

In the study of materials, one encounters the fascinating concept of the dielectric function, which characterizes the material's response to an applied electric field. Let's delve into this intriguing phenomenon and explore its various aspects.

Imagine a point inside the material under investigation, where an externally applied electric field \vec{E} is present. The polarization field \vec{P} is an additional electric field induced at that point by the external field, and is directly proportional to it:

$$\vec{P} = \tilde{\chi} \epsilon_0 \vec{E} \quad (19)$$

Here, $\tilde{\chi}$ is known as the complex electric susceptibility of the material, and ϵ_0 represents the free space dielectric constant. By analyzing Maxwell's equations, we find that the displacement field \vec{D} is a sum of the external electric field and the polarization field:

$$\vec{D} = (1 + \tilde{\chi}) \epsilon_0 \vec{E} \quad (20)$$

Introducing the concept of the complex dielectric function, denoted as $\tilde{\epsilon}$, we establish a constant of proportionality between the displacement and electric fields:

$$\tilde{\epsilon} = (1 + \tilde{\chi}) \epsilon_0 = \tilde{\epsilon}_r \epsilon_0 \quad (21)$$

where $\tilde{\epsilon} = \epsilon_1 - i\epsilon_2$ is the complex dielectric constant of the material, and $\tilde{\epsilon}_r$ represents the complex relative dielectric constant. This leads us to the relationship between the displacement and external electric fields:

$$\vec{D} = \tilde{\epsilon} \vec{E} \quad (22)$$

It is important to consider the isotropic response of the material to the applied field, where the behavior is equal in all directions. However, for materials with non-cubic symmetry, the complex scalar dielectric function in Equation (22) must be replaced with a 3×3 tensor dielectric function.

The complex index of refraction \tilde{N} is closely related to the complex dielectric function $\tilde{\epsilon}$ [15].

$$N^2 = \tilde{\epsilon} \quad (23)$$

Specifically, the real part of the dielectric constant (ϵ_1) and the extinction coefficient (ϵ_2) can be derived from N as follows:

$$\epsilon_1 = n^2 - k^2 \quad (24)$$

$$\epsilon_2 = 2nk$$

Finally,

$$\begin{aligned} n &= \left[\frac{\epsilon_1 + (\epsilon_1^2 + \epsilon_2^2)^{\frac{1}{2}}}{2} \right]^{\frac{1}{2}} \\ k &= \left[\frac{-\epsilon_1 + (\epsilon_1^2 + \epsilon_2^2)^{\frac{1}{2}}}{2} \right]^{\frac{1}{2}} \end{aligned} \quad (25)$$

5. Model of Dielectric Functions

The optical constants n and k , representing the refractive index and the extinction coefficient, respectively, exhibit a wavelength-dependent behavior known as dispersion. In the UV-VIS-NIR range of the electromagnetic spectrum, which is of great interest for spectroscopic ellipsometry, n and k can display complex and intricate variations. While experimental data can be fitted by adjusting n and k values at each wavelength, the modern approach in spectroscopic ellipsometry aims to obtain physically reasonable dispersion models for n and k .

In our manuscript, we predominantly focus on the Cauchy and Lorentz optical models. However, it is essential for readers to note that the field of SE is not confined to these models. There are advanced models which provide detailed insights into various types of materials. For instance, the Tauc–Lorentz and Cody–Lorentz models are designed for amorphous materials. Moreover, other sophisticated models, like the critical points model, the effective medium approximations (EMA), and the Gaussian model are pivotal in deepening our understanding of various other material types, including direct transition semiconductors, composite materials, and disordered systems. These models are tailored for advanced, specialized analysis and contribute to a more profound comprehension of material properties and behaviors. For a more exhaustive exploration of these optical models, we urge readers to delve into specialized literature and resources in the field of SE (See, for example, a detailed discussion of these models in Ref. [7]).

5.1. Cauchy Model

In cases where the dielectric function of a sample is unknown, it becomes essential to model it using an appropriate approach based on the sample's optical properties. For transparent materials with a negligible extinction coefficient ($k \sim 0$, or very small), the Cauchy and the Sellmeier dispersion models are commonly used. This model describes the index of refraction, $n(\lambda)$, with the Cauchy expression, as follows:

$$n(\lambda) = A + \frac{B}{\lambda^2} + \frac{C}{\lambda^4} \quad (26)$$

Alternatively, the “Cauchy–Urbach” model provides a second formulation of the Cauchy model, one which is more suitable for weakly absorbing materials. This model incorporates an exponential absorption tail with the following equation:

$$k(\lambda) = \alpha e^{\beta(1.24\mu m(\frac{1}{\lambda} - \frac{1}{\gamma}))} \quad (27)$$

The six parameters in this dispersion model are A , B , C , the amplitude α , the exponent factor β , and the band edge γ .

While this approach is useful for transparent or nearly transparent materials exhibiting slight absorption at the UV-end of the spectral range, it is less effective for materials with significant absorption, especially if there is an absorption band within the range of interest. Additionally, for metals and semiconductors, Cauchy's formulation lacks physical significance, and these empirical relations are not consistent with the Kramers–Kronig relations [16].

In addition, when encountering materials with substantial absorption bands in the spectral range, particularly those due to molecular vibrations (e.g., C=O stretch) in the in-

frared or electronic vibrations in the ultraviolet, the Cauchy expression alone is inadequate to describe their optical properties.

In such cases, the Lorentz model emerges as a valuable alternative, offering a more comprehensive description of the material's optical behavior. The Lorentz model accounts for the presence of absorption bands and enables a better representation of the optical constants, together with increased accuracy. By employing a physically meaningful model, spectroscopic ellipsometry can provide deeper insights into the behavior of materials and enable more reliable material characterizations for a wide range of applications.

5.2. Lorentz Model

The Lorentz model presents an analogy in which an atom contains electrons that are bound to the nucleus, much as a small mass can be bound to a larger mass by a spring. The equation of motion for an electron bound to the nucleus is described as follows [17]:

$$m \frac{d^2 \vec{r}}{dt^2} + m\Gamma \frac{d\vec{r}}{dt} + m\omega_0^2 \vec{r} = -e\vec{E} \quad (28)$$

In this equation, m represents the electronic mass, e is the magnitude of electronic charge, and \vec{E} is the local electric field acting on the electron as a driving force. The term $m\Gamma \frac{d\vec{r}}{dt}$ accounts for viscous damping, which serves as an energy loss mechanism. In a free atom, this loss mechanism is radiation damping, but in a solid, it arises from various scattering mechanisms. Additionally, the term $m\omega_0^2 \vec{r}$ is a restoring force governed by Hooke's law.

However, there are two approximations made in the standard model expressed in (28). Firstly, the nucleus is assumed to have infinite mass, which implies the use of reduced mass should this not be the case. Secondly, a small force arising from the interaction of the electron with the magnetic field of the light wave is neglected due to the electron's relatively small velocity compared to the speed of light, making it negligible.

The solution to (28) is

$$\hat{r} = \frac{-e\vec{E}/m}{(\omega_0^2 - \omega^2) - i\Gamma\omega} \quad (29)$$

and the induced dipole moment can be expressed as

$$\hat{p} = \frac{e^2}{m} E \frac{1}{(\omega_0^2 - \omega^2) - i\Gamma\omega} \quad (30)$$

In this context, we consider the displacement \hat{r} to be small enough to establish a linear correlation between \hat{p} and E , one represented by the following equation:

$$\hat{p} = \hat{\alpha}(\bar{\omega})E \quad (31)$$

Here, $\hat{\alpha}(\bar{\omega})$ signifies the atomic polarizability, which varies with frequency.

The polarizability is complex because it includes a damping term, resulting in polarization that differs in phase from the local field at all frequencies.

$$\hat{\alpha}(\bar{\omega}) = \frac{e^2}{m} \frac{1}{(\omega_0^2 - \omega^2) - i\Gamma\omega} \quad (32)$$

The complex dielectric constant is given by

$$\hat{\epsilon} = 1 + 4\pi N\hat{\alpha} \quad (33)$$

(N atoms per unit volume).

Using (32) in (33), the complex dielectric constant becomes

$$\hat{\varepsilon} = 1 + \frac{4\pi Ne^2}{m} \frac{1}{(\omega_0^2 - \omega^2) - i\Gamma\omega} \quad (34)$$

Equation (34) can be separated into its real and imaginary parts using (24):

$$\varepsilon_1(\omega) = n^2 - k^2 = 1 + \frac{4\pi Ne^2}{m} \frac{(\omega_0^2 - \omega^2)}{(\omega_0^2 - \omega^2)^2 + \Gamma^2\omega^2} \quad (35)$$

$$\varepsilon_2(\omega) = 2nk = \frac{4\pi Ne^2}{m} \frac{\Gamma\omega}{(\omega_0^2 - \omega^2)^2 + \Gamma^2\omega^2} \quad (36)$$

For normal atoms containing more than one electron per atom, the previous results can be extended. By considering the density of electrons bound N_j with resonance frequency $\bar{\omega}_j$, we can obtain a more comprehensive model.

$$\hat{\varepsilon} = 1 + \frac{4\pi Ne^2}{m} \sum_j \frac{N_j}{(\omega_j^2 - \omega^2) - i\Gamma_j\omega} \quad (37)$$

$$\sum_j N_j = N$$

We can also derive the expressions of n and k in terms of ε_1 and ε_2 :

$$n = \sqrt{\frac{1}{2} \left[(\varepsilon_1^2 + \varepsilon_2^2)^{\frac{1}{2}} + \varepsilon_1 \right]}; \quad k = \sqrt{\frac{1}{2} \left[(\varepsilon_1^2 + \varepsilon_2^2)^{\frac{1}{2}} - \varepsilon_1 \right]} \quad (38)$$

Real materials comprise a collection of oscillators grouped together in the ultraviolet (UV), visible (VIS), and infrared (IR) ranges. The Lorentz oscillator models provide valuable insights into the qualitative aspects of insulators, semiconductors, and conductors by identifying the resonant frequency in the spectral range. The resonant frequency ω_0 is related to the optical band gap (E_g), where $\hbar\omega_0 \cong E_g$ [11].

For insulators or dielectrics, ω_0 lies in the UV range.

Semiconductors require multiple oscillators to be adequately modeled, with ω_0 being close to or within the visible range. The extinction coefficient (k) for semiconductors is small, but nonzero.

As for metals, a great number of conductors exist in which electrons are not bound to specific atoms or locations within the material. These free carriers exhibit distinctive optical absorption, which can be derived by solving for the trajectories of free carriers under the influence of a driving electromagnetic field. Metals can be approximated by the Drude model, a modification of the Lorentz oscillator, in which ω_0 tends to zero due to the negligible restoring force resulting from the absence of a bandgap. The Fermi energy for metals lies within one of the electron energy bands.

6. Kramers–Kronig Relationships

In the field of optical phenomena, the real and imaginary components of the complex index of refraction and complex dielectric function are inherently interconnected, and not independent entities. The Kramers–Kronig relations [16] offer a fundamental connection between these two aspects, one arising from the fundamental principle that a material cannot instantaneously respond to an applied electric field before the field is actually applied. These relationships can be expressed mathematically as follows:

$$n(E) - 1 = \frac{2}{\pi} P \int_0^\infty \frac{E'k(E')}{E'^2 - E^2} dE' \quad (39)$$

$$\varepsilon_1(E) - 1 = \frac{2}{\pi} P \int_0^{\infty} \frac{E' \varepsilon_2(E')}{E'^2 - E^2} dE' \quad (40)$$

In this context, the Lorentz oscillator stands as a model that satisfies Kramers–Kronig consistency, whereas the Cauchy and Urbach relationships remain phenomenological and lack Kramers–Kronig consistency.

7. Applications of Spectroscopic Ellipsometry in Material Science

Spectroscopic ellipsometry has found widespread applications in material science due to its versatility, precision, and non-destructive nature. This section highlights some of the key applications of ellipsometry in various domains of material science, including semiconductor technology, thin film characterization, surface science, and biomaterial analysis.

7.1. Semiconductor Technology

In semiconductor research and device fabrication, ellipsometry plays a pivotal role in determining critical parameters such as layer thickness, composition, and optical properties. It is an indispensable tool for quality control and process monitoring in the semiconductor industry. One of the primary applications of ellipsometry in this field is the characterization of epitaxial thin films [18]. By analyzing the oscillations in ellipsometric parameters, researchers can precisely determine the thickness and interface roughness of thin layers grown on a substrate.

Ellipsometry is also extensively used for the investigation of doping profiles in semiconductors [19]. The incorporation of dopant atoms alters the material's dielectric function, leading to changes in the ellipsometric parameters. This enables researchers to deduce the concentration and depth distribution of dopants, which is critical for designing and optimizing semiconductor devices. This technique introduces dopants into a semiconductor, thereby modulating its electrical properties. However, ion implantation is not without its challenges; it can induce a range of forms of lattice damage, including point defects, dislocations, and, in extreme cases, even amorphization.

Erman et al. [20] studied the dielectric functions of ion-implanted GaAs layers. The authors introduce the harmonic oscillator approximation as an analytical framework to describe these functions. This innovative approach enables the non-destructive determination of damage profiles in ion-implanted materials, thereby providing a robust tool for quality control in semiconductor fabrication.

Ref. [21] demonstrates how ellipsometry can be adapted to study ion-implanted silicon wafers. The authors elucidate the changes in ellipsometric parameters that occur due to ion implantation, as well as the subsequent annealing processes, thereby highlighting the versatility of ellipsometry in studying a range of semiconductor conditions and treatments.

SE was also used to examine the damage profiles in silicon specimens implanted with P⁺, BF₂⁺, As⁺, and B⁺ ions [22]. The effective dielectric functions of the layers subjected to damage are determined employing Bruggeman's effective medium approximation. This approach is based on the assumption that the optical representation of the damaged layer is a combination of crystalline and amorphous silicon. The model's accuracy is enhanced by selectively employing the dielectric function of either implanted or relaxed amorphous silicon as reference data for the amorphous silicon, offering a more precise representation and analysis.

Ellipsometry studies on implanted crystalline substrates highlight the transformation of these substrates into an amorphous state, given the stark difference in optical properties between crystalline and amorphous mediums. Traditional models suggest that this amorphization from ion beams results either from a phase transition due to a high concentration of point defects introduced by individual ions or from the merging of isolated damaged regions. The exact mechanisms of amorphization through ion implantation, however, remain a topic of active research [23].

7.2. Thin Film Characterization

Thin films find applications in various industries, including microelectronics, photovoltaics, optical coatings, and sensors. Accurate characterization of a thin film's properties is crucial for tailoring its performance to specific applications. Ellipsometry provides a non-destructive means of determining a thin film's thickness, refractive index, and extinction coefficient [24].

In the field of microelectronics, ellipsometry is employed to analyze the dielectric properties of gate oxides and passivation layers. For photovoltaic applications, it helps optimize the anti-reflective coatings [25] and measure the thickness and optical constants of different layers in solar cells [26]. Additionally, ellipsometry is widely used in the analysis of organic thin films and the investigation of organic light-emitting diodes (OLEDs) [27].

7.3. Surface Science

Surface properties significantly influence the behavior of materials, especially at the nanoscale. Ellipsometry provides valuable information about surface roughness, adlayer formation, and surface chemistry [9,28]. It is employed in studying self-assembled monolayers (SAMs) on various substrates [29], which finds applications in nanotechnology, biosensors, and corrosion protection [30].

Ellipsometry is also utilized for characterizing biomolecular interactions at interfaces, such as protein adsorption on surfaces [31]. The real-time monitoring capability of ellipsometry allows researchers to study kinetic binding processes, making it an invaluable tool in biomaterial analysis, as will be discussed in Section 7.8.

7.4. Optical Constants and Dielectric Function

Accurate knowledge of the optical constants (refractive index and extinction coefficient) and the dielectric function of materials is essential for designing optical devices and understanding light-matter interactions. SE enables the determination of these parameters over a broad spectral range [32].

By applying models such as the Cauchy or Lorentz dispersion models, ellipsometry can describe the wavelength-dependent behavior of materials. The obtained optical constants can be used to calculate other material properties, such as the bandgap of semiconductors or the plasmonic resonance of metallic nanoparticles [33,34].

7.5. Mueller-Matrix Spectroscopic Ellipsometry

Anisotropic materials are distinguished by their inherent ability to display varied optical properties along different crystallographic directions. This unique optical behavior is a consequence of the specific structural or molecular orientation within the material. For example, in certain crystals, the distinct arrangement of atoms along various axes results in individual refractive indices for each axis.

SE, and more specifically, Mueller-matrix spectroscopic ellipsometry (MMSE), has emerged as a pivotal tool in the study of these materials [35]. MMSE is an advanced optical characterization technique that offers a 4×4 Mueller matrix of a sample. This matrix is instrumental in determining the changes in the state of polarization when light interacts with the sample. The comprehensive nature of the Mueller matrix, accounting for both intensity and polarization changes, makes MMSE especially adept for the study of intricate optical phenomena, such as those presented by anisotropic materials.

The strength of MMSE in studying anisotropy lies in its capability to measure the complete polarization state of light after its interaction with a sample. When polarized light encounters an anisotropic material, its polarization state undergoes complex alterations, which is contingent on the optical properties of the material and the angle of light incidence.

Materials with low dimensions, like 2D materials and quasi-1D crystals, frequently showcase pronounced optical anisotropy. This is often attributed to asymmetries in their lattice structures or their dimensional scales. Moreover, MMSE offers valuable insights into the optical properties of a range of anisotropic materials. This includes understanding

phenomena like birefringence in flexible polymeric substrates or retardance in liquid crystals. By meticulously analyzing the data from the Mueller matrix, researchers may determine factors like the orientation-dependent refractive indices, absorption coefficients, and even the crystal symmetry inherent to anisotropic materials [36].

7.6. Nanomaterials and Nanostructures

In recent advancements in nanotechnology, the detailed study of nanomaterials and nanostructures has become a central focus. SE serves as a crucial tool in this area, facilitating the analysis of the optical properties of nanostructured materials, particularly emphasizing their size-dependent characteristics [37]. This technique is particularly effective in analyzing nanoparticle thin films, a significant component in nanotechnology research. It provides a deep understanding of low-dimensional systems, elucidating the principles of quantum confinement which are fundamental to altering the properties of nanoscale materials. Ellipsometry is also helpful in investigating the effects of particle size on the dielectric response of nanomaterials, a vital factor in the creation of materials for plasmonic applications [38]. It enables the detailed study of metamaterials, offering insights into their nanostructures and dielectric properties. SE has also proven to be essential in the development of detectors with improved accuracy, fostering growth in the field of material science [39].

7.7. In Situ and Real-Time Monitoring

In many material science applications, it is crucial to monitor processes in real time to understand the dynamics and kinetics of structural changes. Ellipsometry can be employed in situ [40] during material growth, deposition, or chemical reactions.

Real-time ellipsometric [41] monitoring enables the determination of growth rates, layer thickness evolution, and optical property changes as materials undergo transformations. This capability is highly advantageous in the development of new materials and for understanding their behavior under various conditions.

7.8. Biomedical Applications of Spectroscopic Ellipsometry

Beyond traditional material science, ellipsometry finds applications in biomedical research. Its non-invasive nature makes it suitable for studying biological samples without the need for extensive sample preparation [42]. Ellipsometry is used to analyze cell adhesion, investigate biomolecular interactions, and monitor the formation of biofilms.

In biomedical implants and prosthetics, ellipsometry aids in characterizing surface coatings to enhance biocompatibility and prevent adverse reactions [43].

SE, known for its precision, is an important tool in the study of biomolecular interactions and the development of new-generation biosensors. Its versatility is evident in its application across various research topics, including protein adsorption studies, cancer biomarker detection, and notably, in the ongoing research into COVID-19.

The COVID-19 pandemic has brought a renewed urgency to the field of biomedical research. In this scenario, SE has been particularly effective in studying how the virus interacts with different surfaces, a line of research that is crucial in the development of materials with antiviral properties and the formulation of preventive strategies [44].

In parallel, SE has been advancing in the study of protein adsorption, offering a deeper understanding of the complex interactions between proteins and nanomaterial surfaces. In fact, when SE is used alongside other methods like electron and fluorescence microscopy, circular dichroism, infrared spectroscopy, AFM, and quartz crystal microbalance, it aids in the study of the microstructure of protein layers adsorbed on material surfaces [31].

In the field of cancer research, a recent study has showcased the potential of SE in the development of geno-sensors for detecting specific cancer biomarkers. For example, Ref. [45] focused on the detection of prostate cancer antigen 3 (PCA3), a biomarker found in the urine of prostate cancer patients. The research highlighted the efficacy of total internal

reflection ellipsometry as a method capable of detecting extremely low concentrations of PCA3.

7.9. *Micro- and Macro-Imaging Ellipsometry*

In the continually evolving field of ellipsometry, the integration of micro- and macro-imaging techniques has substantially enriched the methodology for thin film characterization. Traditional ellipsometry, while proficient in analyzing unstructured surfaces, encounters limitations when applied to the complex micro- and nanostructured devices that are increasingly common in the electronics industry. Ref. [46] addresses this gap by evaluating the utility of imaging and mapping ellipsometry for patterned layers of SiO₂ and photoresist on silicon wafers. Complementing this focus on micro-level applications, Ref. [47] extends the discourse to the field of large-area mapping. Ref. [47] categorizes thin-film characterization methods and emphasizes the suitability of ellipsometry for in-line characterization. This is particularly relevant for industrial applications, such as solar panels and display technology, highlighting the scalability of ellipsometry techniques from micro to macro levels.

However, the field is not without its challenges, especially in the quantitative aspects of imaging ellipsometry (IE). Asinovski et al. [48] argue that with proper calibration and correction, IE can serve as a reliable alternative to classical single-point methods, thereby broadening the methodological scope of ellipsometry.

7.10. *Integration of Auxiliary Surface Characterization Techniques with Spectroscopic Ellipsometry*

It is essential to emphasize the role of auxiliary surface characterization techniques such as AFM, HRSTM, and SEM in combination with SE. Ref. [49] accentuates the importance of utilizing supplementary surface characterization methods like AFM for an all-encompassing insight into the structural and morphological properties of thin films. This study offers a detailed examination of nanocrystalline NiO thin films, showcasing the correlation between the increase in grain size, observable through AFM, and the enhancement of film thickness, which subsequently impacts the optical properties analyzed by SE. The concurrent use of these advanced techniques improves precision and accuracy, which is essential for the advancement of research and development in the field of material science and optical materials. Additionally, Refs. [50–54] further underline the importance of using additional surface characterization techniques with SE.

7.11. *Advantages and Disadvantages of Spectroscopic Ellipsometry*

SE is a powerful optical technique widely employed for the characterization of thin films and layered structures. One of its most remarkable features, particularly in thickness sensitivity, is its high precision, which can reach up to approximately 0.1 Å [15]. This level of precision makes it a vital tool in fields such as semiconductor manufacturing, where even small variations in film thickness can have significant implications. Additionally, the method is nondestructive, allowing for the preservation of the integrity of the sample during analysis. Another advantage of SE is its speed. Measurements can often be completed in just a few seconds, making it highly efficient for real-time monitoring and feedback control during processing. Moreover, this technique can be used in several applications, as discussed in the previous section of this review. The ability for real-time monitoring further enhances its applicability, as it allows for immediate adjustments to be made during experimental or manufacturing processes.

However, SE is not without its drawbacks [15]. One of the most significant limitations is its indirect nature. Unlike some other characterization methods, SE requires the use of an optical model for data analysis. This necessity can complicate the analysis process, particularly when the sample's structure is not well-understood. Constructing an accurate optical model can be challenging and time-consuming, offsetting some of the speed advantages of the technique. Another downside is its relatively low spatial resolution, which is typically in the range of several millimeters. This limitation can be a difficulty in

applications where high spatial resolution is required. Furthermore, the technique faces challenges in characterizing materials with low absorption coefficients ($\alpha < 100 \text{ cm}^{-1}$). This makes it less suitable for certain types of materials and specific applications where low absorption coefficients are of interest.

Despite these limitations, recent advancements like imaging ellipsometry aim to improve spatial resolution, and ongoing research is focused on overcoming some of these intrinsic disadvantages.

8. Conclusions and Outlook

8.1. Conclusions

Throughout this review, we have considered the fundamental principles, data analysis methods, and various applications of spectroscopic ellipsometry.

SE, an advanced non-invasive optical technique, has revolutionized material characterization, providing invaluable insights into the properties of surfaces, interfaces, and thin films. By analyzing the alteration in the polarization state of light upon reflection or transmission through a sample, ellipsometry derives essential parameters such as thin film thickness (t), refractive index (n), and extinction coefficient (k). Its capability to analyze complex multilayered structures and material mixtures makes it an indispensable tool for investigating a wide range of materials, including semiconductors, dielectrics, polymers, and metals.

The name “ellipsometry” is rooted in the elliptical polarization of light that occurs during measurement, and this technique plays a pivotal role in studying materials across various spectral regions. In the ultraviolet/visible (UV/VIS) region, it enables the characterization of interband transitions and provides information about the bandgap (E_g) of materials. Furthermore, in the infrared (IR) region, ellipsometry offers valuable insights into free carrier absorption, lattice vibration modes (LO and TO phonons), and local atomic structures.

This comprehensive review aims to delve into the fundamental principles of ellipsometry, shedding light on the key parameters (Δ and Ψ) measured and their dependence on wavelength and angle of incidence. The Fresnel equations governing the behavior of light at the sample–incident medium interface are discussed in detail, along with the significance of the complex quantity ρ , a term which enables the analysis of rough surfaces, interfaces, and materials with multiple components.

Data analysis methods employed in ellipsometry are thoroughly explored, encompassing the fitting of experimental measurements with theoretical models for precise material characterizations. The Cauchy and Lorentz dispersion models are highlighted for their efficacy in describing diverse materials, including insulators, semiconductors, and metals. Additionally, the Kramers–Kronig relations establish a vital connection between the real and imaginary components of the complex dielectric function, enriching the understanding of material behavior.

Throughout the analysis, the review showcases the diverse applications of spectroscopic ellipsometry, ranging from fundamental research to industrial applications. Its non-contact, non-destructive nature and rapid data acquisition make it an ideal *ex situ* tool for material characterization, allowing for the simulation and generation of application models for an extensive array of materials and unknown combinations.

Moreover, the review delves into the challenges and limitations faced in spectroscopic ellipsometry, such as the need for higher spatial resolution for ultra-thin films (<10 nm) and the measurement of small absorption coefficients, particularly in the UV region. The significance of performing measurements at oblique angles is discussed, especially for anisotropic materials like semiconductors. Additionally, accurate analysis of multilayered samples necessitates prior knowledge of optical constants, which can sometimes be challenging to obtain.

In conclusion, our work provides a comprehensive and insightful overview of ellipsometry, its principles, methodologies, and applications in material characterization. The

versatility, accuracy, and non-destructive nature of ellipsometry position it as an indispensable tool for the study of a wide array of materials, with potential applications spanning fields such as electronics, optoelectronics, thin-film technology, and surface science.

8.2. Outlook

As technological advancements continue to enhance ellipsometers' capabilities, the future prospects of this optical technique are undoubtedly promising, offering unprecedented opportunities for innovative research and development in materials science and beyond. It becomes evident that ellipsometry will continue to play a pivotal role in both scientific research and technological advancements, driving innovation across multiple disciplines.

While SE continues to evolve, the field faces a series of complex challenges and opportunities that could shape its future trajectory. One of the most pressing issues is the need for enhanced accuracy in measurements. This concern extends beyond the capabilities of current instrumentation and calls for a more comprehensive approach to data collection and interpretation.

The limitations of existing optics-based systems are becoming increasingly apparent, particularly in terms of their signal-to-noise ratios [55]. As technological advancements continue to push the boundaries of miniaturization, the challenges associated with metrology are becoming more complex. The transition to smaller nodes, such as the 7 nm node [55], introduces new difficulties in determining both material properties and critical dimensions. This complexity is further compounded by the increasing intricacy of the materials under study.

In terms of process control, the current applications of SE in integrated circuit (IC) technology are primarily in-line [55]. However, the untapped potential for real-time or closed-loop feedback control systems remains significant. The economic feasibility of such advanced control systems will likely depend on the development of specific applications that necessitate them.

Moreover, SE is gradually making its way into the fields of biology and medicine, especially after the COVID-19 pandemic [44]. The study of complex, anisotropic materials presents another promising frontier for SE. The ability to measure the complete Mueller matrix could open up new research avenues for materials previously considered too complex for accurate measurement [56].

Lastly, there is a growing need for improved data management and extraction techniques. The emerging field of reciprocal-space analysis offers a potential solution for intelligently filtering data, thereby enabling more accurate and meaningful interpretations [55].

Another important aspect, one which has not been suggested before, is the growing potential for artificial intelligence (AI) to revolutionize the way we interpret SE data. Given AI's prowess in handling vast datasets and discerning patterns, it can significantly enhance the precision and efficiency of ellipsometry analyses [57]. Machine learning [58,59], when integrated with SE, offers an alternative to intricate optical modeling. The relationship between the thicknesses of individual layers in a multilayer structure and ellipsometric data can be systematically learned through machine learning.

In conclusion, the future of SE is rich with opportunities for methodological advancements and broader applications. However, these opportunities come with their own sets of challenges that will require innovative solutions, interdisciplinary collaboration, and a more integrated approach to data collection and analysis.

Author Contributions: Writing—original draft preparation, G.G.P. and C.V., writing—review and editing, G.G.P. and C.V.; supervision, C.V. All authors have read and agreed to the published version of the manuscript.

Funding: This research received no external funding.

Institutional Review Board Statement: Not applicable.

Informed Consent Statement: Not applicable.

Data Availability Statement: Not applicable.

Conflicts of Interest: The authors declare no conflict of interest.

References

1. Theeten, J.B.; Aspnes, D.E. Ellipsometry in Thin Film Analysis. *Annu. Rev. Mater. Sci.* **1981**, *11*, 97–122. [\[CrossRef\]](#)
2. Zollner, S.; Abadizaman, F.; Emminger, C.; Samarasingha, N. Spectroscopic ellipsometry from 10 to 700 K. *Adv. Opt. Technol.* **2022**, *11*, 117–135. [\[CrossRef\]](#)
3. Riegler, H. A user's guide to ellipsometry. By Harland G. Tompkins, Academic Press, New York 1993, 260 pp. hardback, ISBN 0-12-603050-0. *Adv. Mater.* **1993**, *5*, 778. [\[CrossRef\]](#)
4. Muller, R.H. Definitions and conventions in ellipsometry. *Surf. Sci.* **1969**, *16*, 14–33. [\[CrossRef\]](#)
5. Hajduk, B.; Bednarski, H.; Trzebicka, B. Temperature-Dependent Spectroscopic Ellipsometry of Thin Polymer Films. *J. Phys. Chem. B* **2020**, *124*, 3229–3251. [\[CrossRef\]](#)
6. Woollam, J.A.; Snyder, P.G. Fundamentals and applications of variable angle spectroscopic ellipsometry. *Mater. Sci. Eng. B* **1990**, *5*, 279–283. [\[CrossRef\]](#)
7. J.A. Woollam Co. *WVASE Manual "Guide to Using WVASE32"*; J.A. Woollam Co.: Lincoln, NE, USA, 2010.
8. Woollam, J.A.; Snyder, P.G.; Rost, M.C. Variable angle spectroscopic ellipsometry: A non-destructive characterization technique for ultrathin and multilayer materials. *Thin Solid Films* **1988**, *166*, 317–323. [\[CrossRef\]](#)
9. Vedam, K.; So, S.S. Characterization of real surfaces by ellipsometry. *Surf. Sci.* **1972**, *29*, 379–395. [\[CrossRef\]](#)
10. Schubert, M. *Infrared Ellipsometry on Semiconductor Layer Structures Phonons, Plasmons, and Polaritons*; Springer: Berlin/Heidelberg, Germany, 2005; Volume 209, pp. 1–190.
11. Tompkins, H.; Irene, E.A. *Handbook of Ellipsometry*; William Andrew: Norwich, NY, USA, 2005.
12. Aspnes, D.E.; Theeten, J.B.; Hottier, F. Investigation of effective-medium models of microscopic surface roughness by spectroscopic ellipsometry. *Phys. Rev. B* **1979**, *20*, 3292–3302. [\[CrossRef\]](#)
13. Khardani, M.; Bouaïcha, M.; Bessaïs, B. Bruggeman effective medium approach for modelling optical properties of porous silicon: Comparison with experiment. *Phys. Status Solidi C* **2007**, *4*, 1986–1990. [\[CrossRef\]](#)
14. Veronica, P.R.; Dinescu, M. Spectroscopic ellipsometry. *Rom. Rep. Phys.* **2012**, *64*, 135–142.
15. Fujiwara, H. *Spectroscopic Ellipsometry: Principles and Applications*; John Wiley & Sons: Hoboken, NJ, USA, 2007.
16. Lucarini, V.; Saarinen, J.J.; Peiponen, K.-E.; Vartiainen, E.M. *Kramers-Kronig Relations in Optical Materials Research*; Springer Science & Business Media: Berlin/Heidelberg, Germany, 2005.
17. Wooten, F. *Optical Properties of Solids*; Academic Press: Cambridge, MA, USA, 1972.
18. Bairagi, S.; Hsiao, C.-L.; Magnusson, R.; Birch, J.; Chu, J.P.; Tarntair, F.-G.; Horng, R.-H.; Järrendahl, K. Zinc gallate (ZnGa₂O₄) epitaxial thin films: Determination of optical properties and bandgap estimation using spectroscopic ellipsometry. *Opt. Mater. Express* **2022**, *12*, 3284–3295. [\[CrossRef\]](#)
19. Katzenmeyer, A.M.; Luk, T.S.; Bussmann, E.; Young, S.; Anderson, E.M.; Marshall, M.T.; Ohlhausen, J.A.; Kotula, P.; Lu, P.; Campbell, D.M.; et al. Assessing atomically thin delta-doping of silicon using mid-infrared ellipsometry. *J. Mater. Res.* **2020**, *35*, 2098–2105. [\[CrossRef\]](#)
20. Erman, M.; Theeten, J.B.; Chambon, P.; Kelso, S.M.; Aspnes, D.E. Optical properties and damage analysis of GaAs single crystals partly amorphized by ion implantation. *J. Appl. Phys.* **1984**, *56*, 2664–2671. [\[CrossRef\]](#)
21. Liu, X. *Infrared Spectroscopic Ellipsometry for Ion-Implanted Silicon Wafers*; Basu, S., Ed.; IntechOpen: Rijeka, Croatia, 2011; p. 6. [\[CrossRef\]](#)
22. Lee, S.; Kim, S.Y.K.S.Y.; Oh, S.O.S.-G. Spectro-ellipsometric Studies of Amorphization and Thermal Annealing in Ion-implanted Silicon. *Jpn. J. Appl. Phys.* **1996**, *35*, 5929. [\[CrossRef\]](#)
23. Shamiryan, D.; Likhachev, D. *Spectroscopic Ellipsometry of Ion-Implantation-Induced Damage*; Globalfoundries: Dresden, Germany, 2012; pp. 89–104. [\[CrossRef\]](#)
24. Politano, G.G.; Versace, C. Variable-Angle Spectroscopic Ellipsometry of Graphene-Based Films. *Coatings* **2021**, *11*, 462. [\[CrossRef\]](#)
25. Rajan, G.; Karki, S.; Collins, R.W.; Podraza, N.J.; Marsillac, S. Real-Time Optimization of Anti-Reflective Coatings for CIGS Solar Cells. *Materials* **2020**, *13*, 4259. [\[CrossRef\]](#) [\[PubMed\]](#)
26. Márquez, E.; Blanco, E.; García-Gurrea, M.; Puerta, M.C.; Domínguez de la Vega, M.; Ballester, M.; Manuel, J.M.; Rodríguez-Tapiador, M.I.; Fernández, S.M. Optical Properties of Reactive RF Magnetron Sputtered Polycrystalline Cu₃N Thin Films Determined by UV/Visible/NIR Spectroscopic Ellipsometry: An Eco-Friendly Solar Light Absorber. *Coatings* **2023**, *13*, 1148. [\[CrossRef\]](#)
27. Gioti, M. Spectroscopic Ellipsometry Studies on Solution-Processed OLED Devices: Optical Properties and Interfacial Layers. *Materials* **2022**, *15*, 9077. [\[CrossRef\]](#)
28. Blanco, J.R.; McMarr, P.J.; Vedam, K. Roughness measurements by spectroscopic ellipsometry. *Appl. Opt.* **1985**, *24*, 3773–3779. [\[CrossRef\]](#)

29. Yeung, C.L.; Charlesworth, S.; Iqbal, P.; Bowen, J.; Preece, J.A.; Mendes, P.M. Different formation kinetics and photoisomerization behavior of self-assembled monolayers of thiols and dithiolanes bearing azobenzene moieties. *Phys. Chem. Chem. Phys.* **2013**, *15*, 11014–11024. [[CrossRef](#)]
30. Canepa, M.; Maidecchi, G.; Toccafondi, C.; Cavalleri, O.; Prato, M.; Chaudhari, V.; Esaulov, V.A. Spectroscopic ellipsometry of self assembled monolayers: Interface effects. The case of phenyl selenide SAMs on gold. *Phys. Chem. Chem. Phys.* **2013**, *15*, 11559–11565. [[CrossRef](#)] [[PubMed](#)]
31. Mora, M.F.; Wehmeyer, J.L.; Synowicki, R.; Garcia, C.D. *Investigating Protein Adsorption via Spectroscopic Ellipsometry BT—Biological Interactions on Materials Surfaces: Understanding and Controlling Protein, Cell, and Tissue Responses*; Puleo, D.A., Bizios, R., Eds.; Springer: New York, NY, USA, 2009; pp. 19–41. [[CrossRef](#)]
32. Politano, G.G.; Castriota, M.; De Santo, M.P.; Pipita, M.M.; Desiderio, G.; Vena, C.; Versace, C. Variable angle spectroscopic ellipsometry characterization of spin-coated MoS₂ films. *Vacuum* **2021**, *189*, 110232. [[CrossRef](#)]
33. Politano, G.G.; Cazzanelli, E.; Versace, C.; Vena, C.; De Santo, M.P.; Castriota, M.; Ciuchi, F.; Bartolino, R. Graphene oxide on magnetron sputtered silver thin films for SERS and metamaterial applications. *Appl. Surf. Sci.* **2018**, *427*, 927–933. [[CrossRef](#)]
34. Politano, G.G.; Vena, C.; Desiderio, G.; Versace, C. Spectroscopic ellipsometry investigation of the optical properties of graphene oxide dip-coated on magnetron sputtered gold thin films. *J. Appl. Phys.* **2018**, *123*, 055303. [[CrossRef](#)]
35. Hilfiker, J.N.; Hong, N.; Schoeche, S. Mueller matrix spectroscopic ellipsometry. *Adv. Opt. Technol.* **2022**, *11*, 59–91. [[CrossRef](#)]
36. Chen, X.; Gu, H.; Jiamin, L.; Chen, C.; Liu, S. Advanced Mueller matrix ellipsometry: Instrumentation and emerging applications. *Sci. China Technol. Sci.* **2022**, *65*, 2007–2030. [[CrossRef](#)]
37. Chattopadhyay, K.K.; Das, N.S. *Size-Dependant Optical Properties of Nanoparticles Analyzed by Spectroscopic Ellipsometry BT—Handbook of Nanoparticles*; Aliofkhazraei, M., Ed.; Springer International Publishing: Cham, Switzerland, 2016; pp. 265–293. [[CrossRef](#)]
38. Oates, T.W.H.; Wormeester, H.; Arwin, H. Characterization of plasmonic effects in thin films and metamaterials using spectroscopic ellipsometry. *Prog. Surf. Sci.* **2011**, *86*, 328–376. [[CrossRef](#)]
39. Toudert, J. Spectroscopic ellipsometry for active nano- and meta-materials. *Nanotechnol. Rev.* **2014**, *3*, 223–245. [[CrossRef](#)]
40. Hilfiker, J.N. 5—*In Situ Spectroscopic Ellipsometry (SE) for Characterization of Thin Film Growth*; Woodhead Publishing Series in Electronic and Optical Materials; Woodhead Publishing: Sawston, UK, 2011; pp. 99–151. [[CrossRef](#)]
41. Mukherjee, D.; Petrik, P. Real-Time Ellipsometry at High and Low Temperatures. *ACS Omega* **2023**, *8*, 3684–3697. [[CrossRef](#)]
42. Jin, G.; Meng, Y.H.; Liu, L.; Niu, Y.; Chen, S.; Cai, Q.; Jiang, T.J. Development of biosensor based on imaging ellipsometry and biomedical applications. *Thin Solid Films* **2011**, *519*, 2750–2757. [[CrossRef](#)]
43. Arwin, H. Application of ellipsometry techniques to biological materials. *Thin Solid Films* **2011**, *519*, 2589–2592. [[CrossRef](#)]
44. Plikusiene, I.; Maciulis, V.; Juciute, S.; Ramanavicius, A.; Balevicius, Z.; Slibinskas, R.; Kucinskaite-Kodze, I.; Simanavicius, M.; Balevicius, S.; Ramanaviciene, A. Investigation of SARS-CoV-2 nucleocapsid protein interaction with a specific antibody by combined spectroscopic ellipsometry and quartz crystal microbalance with dissipation. *J. Colloid Interface Sci.* **2022**, *626*, 113–122. [[CrossRef](#)] [[PubMed](#)]
45. Takita, S.; Nabok, A.; Smith, D.; Lishchuk, A. Spectroscopic Ellipsometry Detection of Prostate Cancer Bio-Marker PCA3 Using Specific Non-Labeled Aptamer: Comparison with Electrochemical Detection. *Chem. Proc.* **2021**, *5*, 65. [[CrossRef](#)]
46. Rosu, D.; Petrik, P.; Rattmann, G.; Schellenberger, M.; Beck, U.; Hertwig, A. Optical characterization of patterned thin films. *Thin Solid Films* **2014**, *571*, 601–604. [[CrossRef](#)]
47. Petrik, P.; Fried, M. Mapping and Imaging of Thin Films on Large Surfaces. *Phys. Status Solidi* **2022**, *219*, 2100800. [[CrossRef](#)]
48. Asinovski, L.; Beaglehole, D.; Clarkson, M.T. Imaging ellipsometry: Quantitative analysis. *Phys. Status Solidi* **2008**, *205*, 764–771. [[CrossRef](#)]
49. Emam-Ismael, M.; El-Hagary, M.; El-Sherif, H.M.; El-Naggar, A.M.; El-Nahass, M.M. Spectroscopic ellipsometry and morphological studies of nanocrystalline NiO and NiO/ITO thin films deposited by e-beams technique. *Opt. Mater.* **2021**, *112*, 110763. [[CrossRef](#)]
50. Emam-Ismael, M.; El-Hagary, M.; Shaaban, E.R.; Moustafa, S.H.; Gad, G.M.A. Spectroscopic ellipsometry and morphological characterizations of nanocrystalline Hg_{1-x}MnxO oxide diluted magnetic semiconductor thin films. *Ceram. Int.* **2019**, *45*, 8380–8387. [[CrossRef](#)]
51. Singh, A.K.; Yadav, B.S.; Vishwakarma, A.K.; Kumar, S.; Ahmad, F.; Kumar, P.; Kumar, N. Spectroscopic Ellipsometry Study of Thermally Evaporated Tin Telluride (SnTe) Thin Films. *J. Electron. Mater.* **2023**, *52*, 7132–7142. [[CrossRef](#)]
52. Potočník, T.; Burton, O.; Reutzel, M.; Schmitt, D.; Bange, J.P.; Mathias, S.; Geisenhof, F.R.; Weitz, R.T.; Xin, L.; Joyce, H.J.; et al. Fast Twist Angle Mapping of Bilayer Graphene Using Spectroscopic Ellipsometric Contrast Microscopy. *Nano Lett.* **2023**, *23*, 5506–5513. [[CrossRef](#)] [[PubMed](#)]
53. Leigh, W.; Mandal, S.; Cuenca, J.A.; Wallis, D.; Hinz, A.M.; Oliver, R.A.; Thomas, E.L.H.; Williams, O. Monitoring of the Initial Stages of Diamond Growth on Aluminum Nitride Using In Situ Spectroscopic Ellipsometry. *ACS Omega* **2023**, *8*, 30442–30449. [[CrossRef](#)] [[PubMed](#)]
54. Gangwar, M.S.; Agarwal, P. Influence of microstructure on dielectric function and plasmonic properties of silver nanoparticles grown by solid state dewetting: A spectroscopic ellipsometry study. *Phys. Scr.* **2023**, *98*, 105944. [[CrossRef](#)]
55. Aspnes, D.E. Spectroscopic ellipsometry—Past; present; future. *Thin Solid Films* **2014**, *571*, 334–344. [[CrossRef](#)]

56. Vala, D.; Mičica, M.; Cvejn, D.; Postava, K. Broadband Mueller ellipsometer as an all-in-one tool for spectral and temporal analysis of mutarotation kinetics. *RSC Adv.* **2023**, *13*, 6582–6592. [[CrossRef](#)] [[PubMed](#)]
57. Wang, H.; Fu, T.; Du, Y.; Gao, W.; Huang, K.; Liu, Z.; Chandak, P.; Liu, S.; Van Katwyk, P.; Deac, A.; et al. Scientific discovery in the age of artificial intelligence. *Nature* **2023**, *620*, 47–60. [[CrossRef](#)]
58. Arunachalam, A.; Berriel, S.N.; Banerjee, P.; Basu, K. Machine learning-enhanced efficient spectroscopic ellipsometry modeling. *arXiv* **2022**, arXiv:2201.04933.
59. Liu, J.; Zhang, D.; Yu, D.; Ren, M.; Xu, J. Machine learning powered ellipsometry. *Light Sci. Appl.* **2021**, *10*, 55. [[CrossRef](#)]

Disclaimer/Publisher's Note: The statements, opinions and data contained in all publications are solely those of the individual author(s) and contributor(s) and not of MDPI and/or the editor(s). MDPI and/or the editor(s) disclaim responsibility for any injury to people or property resulting from any ideas, methods, instructions or products referred to in the content.